

Holographic anisotropic background with confinement-deconfinement phase transition

Kristina Rannu^{1,*}

¹Peoples' Friendship University of Russia, Miklukho-Maklaya str.6, 117198, Moscow, Russia

Abstract. We present new anisotropic black brane solutions in 5D Einstein-dilaton-two-Maxwell system [1]. The anisotropic background is specified by an arbitrary dynamical exponent ν , a nontrivial warp factor, a non-zero dilaton field, a non-zero time component of the first Maxwell field and a non-zero longitudinal magnetic component of the second Maxwell field. The blackening function supports the Van der Waals-like phase transition between small and large black holes for a suitable first Maxwell field charge. The isotropic case corresponding to $\nu = 1$ and zero magnetic field reproduces previously known solutions. We investigate the anisotropy influence on the thermodynamic properties of our background, in particular, on the small/large black holes phase transition diagram.

1 Introduction

Accepting holographical approach to quark-gluon plasma (QGP) we need natural theory with metric as solution of EOM. The most interesting holographic phenomenology, describing heavy ions collisions (HIC), is related with the model containing vector field responsible $\mu \neq 0$, that allows to restore phase transition diagram in temperature-chemical potential plane $T(\mu)$ [2, 3]. For these purposes the following metric is well suited [4]:

$$ds^2 = L^2 \frac{b(z)}{z^2} \left[-g(z) dt^2 + dx^2 + z^{2-\frac{2}{\nu}} (dy_1^2 + dy_2^2) + \frac{dz^2}{g(z)} \right], \quad (1)$$

where $b(z)$ is the warp factor, $g(z)$ is the blackening function and ν is the anisotropy index; we set the AdS radius $L = 1$ and all the quantities in formulas and figures are presented in dimensionless units.

In this work we consider the black brane solution in the anisotropic background, using the metric ansatz (1). This metric is a generalization of a so called AGG solution [5]:

$$ds^2 = \frac{L^2}{z^2} \left[-g(z) dt^2 + dx^2 + z^{2-\frac{2}{\nu}} (dy_1^2 + dy_2^2) + \frac{dz^2}{g(z)} \right], \quad (2)$$

where $b(z) = 1$ and $\mu = 0$.

*e-mail: rannu_ka@pfur.ru

Main interest for the AGG-metric is that in zero chemical potential case

- for $g(z) = 1$ the shock wave collision in this background under some conditions produces a black hole and the entropy of this BH gives the correct energy dependence of multiplicity,
- for $g(z) \neq 1$ it describes the thermodynamics of QGP produced in HIC.

Our goal is to get the generalizations of these results to non-zero chemical potential, that is important for the expected study of $T(\mu)$ -phase transition diagram on NICA. In this work we also followed the Yang and Yuan articles [6, 7]. Their solution was isotropic but included the non-zero chemical potential.

2 Black brane anisotropic solution

The AGG-metric (2) in [5] has been constructed as solution to EOM for the Einstein-dilaton-Maxwell Lagrangian. To expand it we add into the Lagrangian an extra Maxwell tensor and therefore consider a 5-dimensional Einstein-dilaton-two-Maxwell system. In the Einstein frame the action of the system is specified as

$$S = \int \frac{d^5x}{16\pi G_5} \sqrt{-\det(g_{\mu\nu})} \left[R - \frac{f_1(\phi)}{4} F_{(1)}^2 - \frac{f_2(\phi)}{4} F_{(2)}^2 - \frac{1}{2} \partial_\mu \phi \partial^\mu \phi - V(\phi) \right], \quad (3)$$

$$A_\mu^{(1)} = A_t(z) \delta_\mu^0, \quad \phi = \phi(z), \quad (4)$$

where $F_{(1)}^2$ and $F_{(2)}^2$ are the squares of the Maxwell fields $F_{\mu\nu}^{(1)} = \partial_\mu A_\nu - \partial_\nu A_\mu$ and $F_{\mu\nu}^{(2)} = q dy^1 \wedge dy^2$, $f_1(\phi)$ and $f_2(\phi)$ are the gauge kinetic functions associated with the corresponding Maxwell fields, $V(\phi)$ is the potential of the scalar field ϕ . Boundary conditions

$$A_t(0) = \mu, \quad A_t(z_h) = 0, \quad g(0) = 1, \quad g(z_h) = 0, \quad \phi(z_h) = 0 \quad (5)$$

provide us with the non-zero chemical potential.

Six independent equations of motion were derived from the Lagrangian (3):

$$g'' + g' \left(\frac{3b'}{2b} - \frac{1}{z} - \frac{2}{vz} \right) - \frac{z^2}{b} f_1 A_t'^2 = 0, \quad (6)$$

$$b'' - \frac{3b'^2}{2b} + \frac{2b'}{z} - \frac{4b}{3vz^2} \left(1 - \frac{1}{v} \right) + \frac{b}{3} \phi'^2 = 0, \quad (7)$$

$$2g' \left(1 - \frac{1}{v} \right) + g \left(1 - \frac{1}{v} \right) \left(\frac{3b'}{b} - \frac{4}{z} - \frac{4}{vz} \right) + \frac{q^2 z^{-1+\frac{4}{v}}}{b} f_2 = 0, \quad (8)$$

$$-V - \frac{z^4}{2b^2} A_t'^2 f_1 - \frac{3z^2 b' g'}{2b^2} - \frac{3z^2 g b'^2}{b^3} + \frac{9z g b'}{2v b^2} + \frac{15z g b'}{2b^2} + \frac{z g'}{v b} + \frac{2z g'}{b} + \frac{z^2 g \phi'^2}{2b} - \frac{8g}{v b} - \frac{4g}{b} = 0, \quad (9)$$

$$A_t'' + A_t' \left(\frac{b'}{2b} + \frac{f_1'}{f_1} - \frac{2-v}{vz} \right) = 0, \quad (10)$$

$$\phi'' + \phi' \left(\frac{g'}{g} + \frac{3b'}{2b} - \frac{v+2}{vz} \right) + \frac{z^2 A_t'^2}{2bg} \frac{\partial f_1}{\partial \phi} - \frac{q^2 z^{-2+\frac{4}{v}}}{2bg} \frac{\partial f_2}{\partial \phi} - \frac{b}{z^2 g} \frac{\partial V}{\partial \phi} = 0, \quad (11)$$

where $' = d/dz$. First five of them give us the required functions A_t , g , ϕ , f_2 and V . The sixth one serves as the constraint.

The most general solution of our EOMs was obtained in assumption that the warp factor is the exponent of some polinom of z coordinate, that generalizes phenomenological factor advocated by Andreev and Zakharov [8], i.e. $b(z) = \exp P(z)$ and ν is non-trivial ($\nu \neq 1$):

$$f_1 = z^{-2+\frac{2}{\nu}}, \tag{12}$$

$$A_t = \tilde{\mu} \int_z^{z_h} e^{-\frac{P(\xi)}{2}} \xi d\xi, \quad \tilde{\mu} = \frac{\mu}{\int_0^{z_h} e^{-\frac{P(\xi)}{2}} \xi d\xi}, \tag{13}$$

$$g = 1 + \tilde{\mu}^2 \int_0^z e^{-\frac{3P(\xi)}{2}} \left(\int_0^\xi e^{-\frac{P(\chi)}{2}} \chi d\chi \right) \xi^{1+\frac{2}{\nu}} d\xi - \frac{1 + \tilde{\mu}^2 \int_0^{z_h} e^{-\frac{3P(\xi)}{2}} \left(\int_0^\xi e^{-\frac{P(\chi)}{2}} \chi d\chi \right) \xi^{1+\frac{2}{\nu}} d\xi}{\int_0^{z_h} e^{-\frac{3P(\xi)}{2}} \xi^{1+\frac{2}{\nu}} d\xi} \int_0^z e^{-\frac{3P(\xi)}{2}} \xi^{1+\frac{2}{\nu}} d\xi, \tag{14}$$

$$\phi = C_5 + \int_0^z \sqrt{-3P''(\xi) + \frac{3}{2}P'^2(\xi) - \frac{6}{\xi}P'(\xi) + 4\frac{\nu-1}{\xi^2\nu^2}} d\xi. \tag{15}$$

The more concrete solution can be obtained for $b = \exp(cz^2/2)$ with the numerical coefficient c :

$$f_1 = z^{-2+\frac{2}{\nu}}, \tag{16}$$

$$A_t = \mu \frac{e^{-\frac{cz^2}{4}} - e^{-\frac{cz_h^2}{4}}}{1 - e^{-\frac{cz_h^2}{4}}}, \tag{17}$$

$$g = 1 - \frac{z^{2+\frac{2}{\nu}}}{z_h^{2+\frac{2}{\nu}}} \frac{\mathfrak{G}(\frac{3}{4}cz^2)}{\mathfrak{G}(\frac{3}{4}cz_h^2)} - \frac{\mu^2 cz^{2+\frac{2}{\nu}} e^{\frac{cz^2}{2}}}{4\left(1 - e^{-\frac{cz_h^2}{4}}\right)^2} \mathfrak{G}(cz^2) + \frac{\mu^2 cz^{2+\frac{2}{\nu}} e^{\frac{cz_h^2}{2}}}{4\left(1 - e^{-\frac{cz_h^2}{4}}\right)^2} \frac{\mathfrak{G}(\frac{3}{4}cz^2)}{\mathfrak{G}(\frac{3}{4}cz_h^2)} \mathfrak{G}(cz_h^2), \tag{18}$$

$$\mathfrak{G}(x) = x^{-1-\frac{1}{\nu}} \gamma\left(1 + \frac{1}{\nu}, x\right) = \sum_{n=0}^{\infty} \frac{(-1)^n x^n}{n!(1+n+\frac{1}{\nu})}, \tag{19}$$

$$\phi = \frac{1}{2\sqrt{2}\nu} \left\{ \sqrt{3c^2\nu^2z^4 - 18c\nu^2z^2 + 8(\nu-1)} - \sqrt{3c^2\nu^2z_h^4 - 18c\nu^2z_h^2 + 8(\nu-1)} + 2\sqrt{2(\nu-1)} \ln\left(\frac{z^2}{z_h^2}\right) - 3\sqrt{3}\nu \ln\left(\frac{\sqrt{3c^2\nu^2z^4 - 18c\nu^2z^2 + 8(\nu-1)} - \sqrt{3}\nu(3-cz^2)}{\sqrt{3c^2\nu^2z_h^4 - 18c\nu^2z_h^2 + 8(\nu-1)} - \sqrt{3}\nu(3-cz_h^2)}\right) - 2\sqrt{2(\nu-1)} \ln\left(\frac{9c\nu^2z^2 - 8(\nu-1) - \sqrt{2(\nu-1)}\sqrt{3c^2\nu^2z^4 - 18c\nu^2z^2 + 8(\nu-1)}}{9c\nu^2z_h^2 - 8(\nu-1) - \sqrt{2(\nu-1)}\sqrt{3c^2\nu^2z_h^4 - 18c\nu^2z_h^2 + 8(\nu-1)}}\right) \right\}. \tag{20}$$

The dilaton function ϕ has non-trivial form and can become complex for $c > 0$, whereas $c < 0$ provides stable solution.

Fig. 1 shows the dependence of the blackening function from the chemical potential. We see that when μ becomes larger than 2 the size of the first horizon decreases and the second horizon becomes physical.

We also got the explicit analytical solution for scalar field potential V (Fig. 2). This expression is too large, but it can be approximated by two exponents, depending on scalar field ϕ and chemical potential μ :

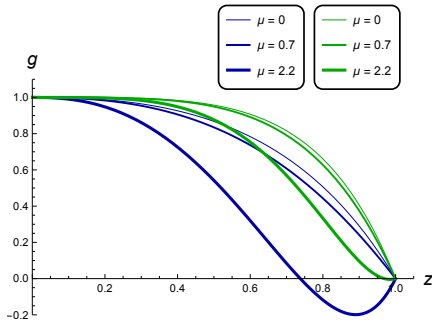


Figure 1. Dependence of the blackening function $g(z)$ from the chemical potential μ for the anisotropic case $\nu = 4.5$ (blue lines) and the isotropic case $\nu = 1$ (green lines), $c = -1$.

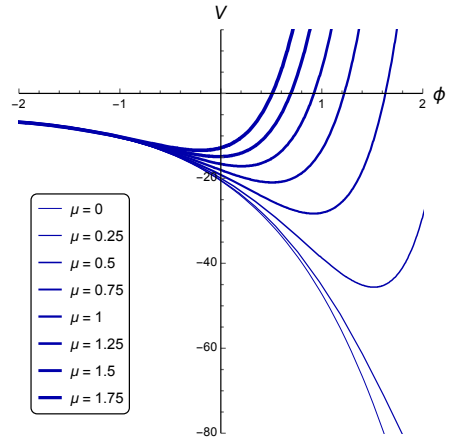


Figure 2. Dependence of the scalar field potential V from the scalar field ϕ for different values of chemical potential μ in the anisotropic case $\nu = 4.5$, $c = -1$.

$$\begin{aligned}
 V(\phi, \mu, \nu) &\approx V_0(\nu) - C_7(\mu, \nu)e^{K_1(\nu)\phi} + C_8(\mu, \nu)e^{K_2(\nu)\phi}, \\
 V_0(4.5) &= -0.5778, \quad K_1(4.5) = 0.7897, \quad K_2(4.5) = 2.0995, \\
 C_7(\mu, 4.5) &= 23.0779 + 2.4236\mu^2, \quad C_8(\mu, 4.5) = 0.0575 + 4.9919\mu^2.
 \end{aligned}
 \tag{21}$$

For trivial warp factor $b(z) = 1$ the solution degenerates in such a way:

$$\begin{aligned}
 f_1 &= z^{-2+\frac{2}{\nu}}, \\
 A_t(z) &= \mu \left(1 - \frac{z^2}{z_h^2} \right), \\
 g(z) &= 1 - \left(\frac{z}{z_h} \right)^{2+\frac{2}{\nu}} \left[1 + \frac{\mu^2 \nu z_h^{\frac{2}{\nu}}}{1 + 2\nu} \left(1 - \frac{z^2}{z_h^2} \right) \right], \\
 \phi &= 2 \frac{\sqrt{\nu-1}}{\nu} \log z + C_5.
 \end{aligned}
 \tag{22}$$

If we also turn off the Maxwell field that provides the chemical potential, we really do obtain the AGG solution back:

$$\begin{aligned}
 g(z) &= 1 - \left(\frac{z}{z_h} \right)^{2+\frac{2}{\nu}}, \\
 f_2(z) &= \frac{4z^{-4/\nu}}{q^2} \frac{(\nu-1)(1+3\nu+2\nu^2)}{\nu^2(1+2\nu)}, \\
 \phi(z) &= C_5 \pm 2 \frac{\sqrt{\nu-1}}{\nu} \log(z), \\
 V(z) &= -2 \frac{(1+\nu)(1+2\nu)}{\nu^2}.
 \end{aligned}
 \tag{23}$$

3 Properties of black brane anisotropic solution

3.1 RG-flow

Following the works by Gursoy, Kiritis et al. [9] (see also [10]), we obtained the renorm-group flow equations. To get the anisotropic case with chemical potential we made the variable change $z \rightarrow w$ and used the following ansatz of the metric:

$$ds^2 = -B(w)^2 g(w) dt^2 + B(w)^2 dx^2 + R(w) (dy_1^2 + dy_2^2) + \frac{dw^2}{g(w)}. \quad (24)$$

Further we introduce functions of the scalar field ϕ :

$$X(\phi) = \frac{B}{B'} \frac{\phi'}{3}, \quad Y(\phi) = \frac{1}{4} \frac{g'}{g} \frac{B}{B'}, \quad Z(\phi) = \frac{1}{4} \frac{R'}{R} \frac{B}{B'} \quad (25)$$

$$H_1(\phi) = \frac{A'}{B}, \quad H_2(\phi) = \frac{q}{R} \quad (26)$$

and write down the renorm-group equations in this form:

$$\begin{aligned} \frac{dX}{d\phi} &= -\frac{2}{9} \mathcal{Z} \left(1 + \frac{1}{X} \frac{2\partial_\phi V - H_1^2 \partial_\phi f_1 + H_2^2 \partial_\phi f_2 - 2XH_2^2 f_2}{2V + H_1^2 f_1 + H_2^2 f_2} \right), \\ \frac{dY}{d\phi} &= -\frac{2Y}{9X} \mathcal{Z} \left(1 + \frac{1}{2Y} \frac{3H_1^2 f_1 - 4YH_2^2 f_2}{2V + H_1^2 f_1 + H_2^2 f_2} \right), \\ \frac{dZ}{d\phi} &= \frac{1-2Z}{9X} \mathcal{Z} \left(1 + \frac{1+4Z}{1-2Z} \frac{H_2^2 f_2}{2V + H_1^2 f_1 + H_2^2 f_2} \right), \\ \frac{dH_1}{d\phi} &= -\left(\frac{1+4Z}{3X} + \frac{\partial_\phi f_1}{f_1} \right) H_1, \\ \frac{dH_2}{d\phi} &= -\frac{4Z}{3X} H_2, \\ \mathcal{Z} &= 1 - \frac{9}{4} X^2 + 2Y + 8Z + 8YZ + 4Z^2. \end{aligned} \quad (27)$$

The particular case of these equations for $\nu = 1$ was published in [1].

3.2 Thermodynamics of the background

Some thermodynamical consideration was performed as well. Here are the expressions for the entropy and the temperature of the black hole.

$$s = \frac{e^{-\frac{3cz_h^2}{4}}}{4z_h^{1+\frac{2}{\nu}}}, \quad (28)$$

$$T = \frac{e^{-\frac{3cz_h^2}{4}}}{2\pi z_h} \left| \frac{1}{\mathfrak{G}(\frac{3}{4} cz_h^2)} + \frac{\mu^2 cz_h^{2+\frac{2}{\nu}} e^{\frac{cz_h^2}{4}}}{4 \left(1 - e^{\frac{cz_h^2}{4}}\right)^2} \left(1 - e^{\frac{cz_h^2}{4}} \frac{\mathfrak{G}(cz_h^2)}{\mathfrak{G}(\frac{3}{4} cz_h^2)} \right) \right|. \quad (29)$$

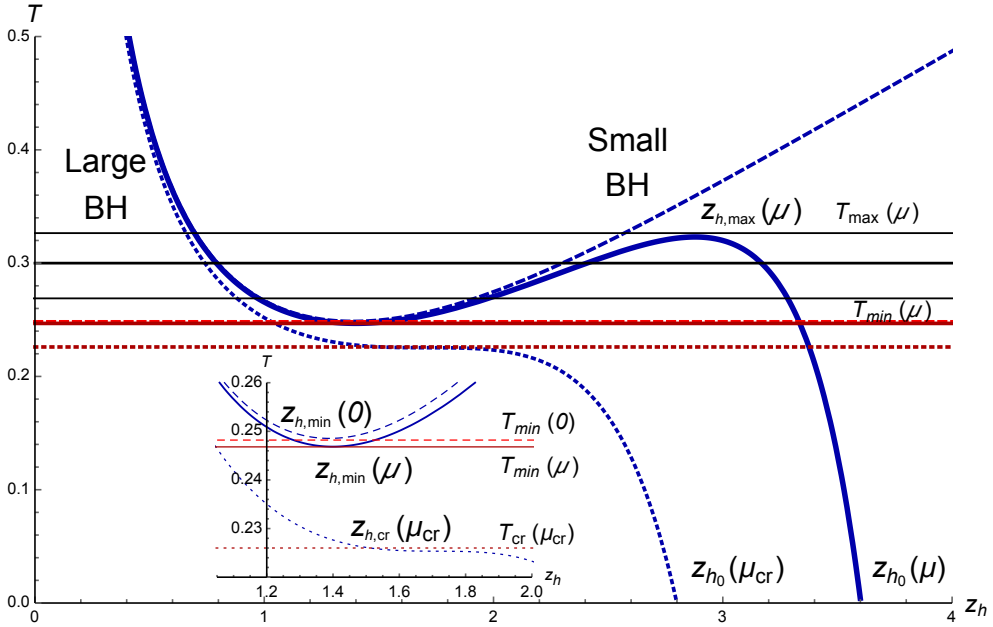


Figure 3. Dependence of the temperature T from the the horizon z_h for different values of chemical potential μ : $\mu = 0$ (dashed lines), $0 < \mu < \mu_{cr}$ (solid lines) and $\mu = \mu_{cr}$ (dotted lines) in the anisotropic case $\nu = 4.5$, $c = -1$; the horizontal orange and red lines show locations of the global minima in isotropic and anisotropic cases, respectively.

Depending on chemical potential we get three main cases of the temperature behavior (Fig. 3). For $\mu = 0$ (dashed lines) there is one extremal point $(z_{h,min}(0); T_{min})$. For $0 < \mu < \mu_{cr}$ (solid lines) there are two extremal points $(z_{h,min}(\mu); T_{min})$ and $(z_{h,max}; T_{max})$. Here z_{h_0} is the position of the new horizon, $T(z_{h_0}) = 0$. For $\mu = \mu_{cr}$ (dotted lines) there is no extremal point, but there is an inflection point $(z_{h,cr}, T_{cr})$, $z_{h,cr} = z_{h,cr}(\mu_{cr})$, $T_{cr} = T_{cr}(\mu_{cr})$, therefore for all values of z_h with its growth the temperature decreases and the temperature becomes equal to zero at a new horizon. For $\mu > \mu_{cr}$ increasing z_h we decrease the temperature and there is a point $z_{h_0} = z_{h_0}(\mu, c, \nu)$ where $T(z_{h_0}) = 0$, i.e. a new horizon appears. For $c = -1$, $\nu = 4.5$ critical value of chemical potential approximately is $\mu \approx 0.35$.

3.3 Confinement-deconfinement phase transition

We also investigated the question of confinement-deconfinement phase-transition. Here are the equations of the position of the domain-walls for our solution:

$$\begin{aligned} \mathcal{D}W_x &\equiv cz + \frac{1}{\nu z} \sqrt{\frac{2}{3}} \sqrt{3c \nu^2 z^2 \left(\frac{cz^2}{2} - 3 \right) + 4\nu - 4} + \frac{g'}{2g} - \frac{2}{z} \Big|_{z=z_{DWx}} = 0, \\ \mathcal{D}W_y &\equiv cz + \frac{1}{\nu z} \sqrt{\frac{2}{3}} \sqrt{3c \nu^2 z^2 \left(\frac{cz^2}{2} - 3 \right) + 4\nu - 4} + \frac{g'}{2g} - \frac{\nu + 1}{\nu z} \Big|_{z=z_{DWy}} = 0. \end{aligned} \quad (30)$$

The form of these equations depends on quark-antiquark orientation so we can clearly see the influence of anisotropy. Using these equations we obtained the diagram for confinement-deconfinement phase transition (Fig. 4).

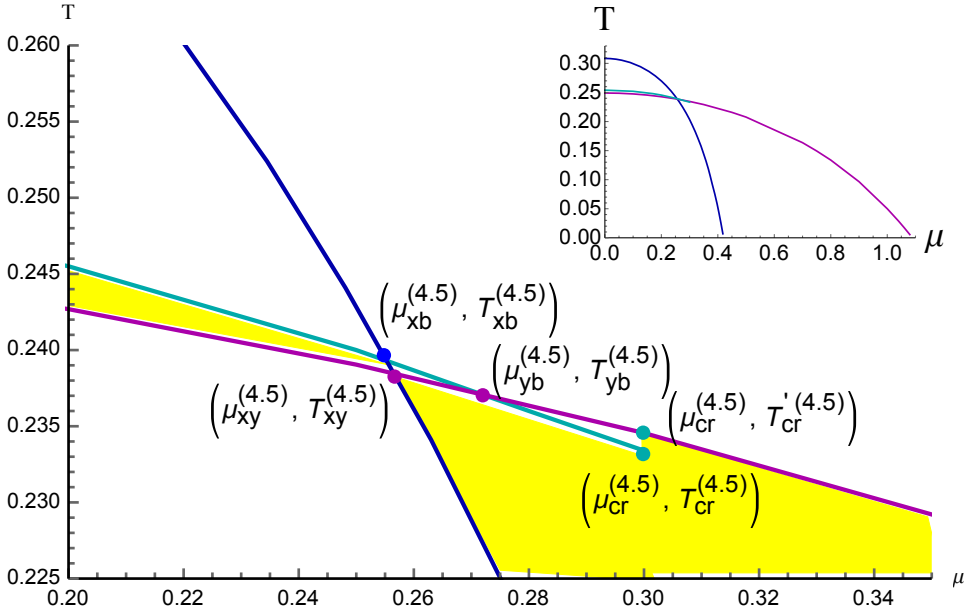


Figure 4. Phase transition diagram for the longitudinal Wilson line W_x (blue line), the transversal lines W_y (magenta line) of the anisotropic case, $\nu = 4.5$, and for the Hawking-Page phase transition of the anisotropic background (cyan line), $c = -1$; top (small) plot shows the general picture, bottom (large) plot shows the intersection region in details.

For $\mu = 0$ temperature corresponding to x direction is larger than in the y direction case. On the other hand for x direction the phase transition line reaches zero temperature at lesser values of chemical potential. The longitudinal orientation parts of regions near zero values of the chemical potential enter to the instability regions of our background, where the small black holes collapse to large ones. Here the horizon suddenly blows up to pass the critical value, so that the confinement phase transforms to the deconfinement one by a phase transition. While the chemical potential is greater than the critical value, the black hole horizon grows gradually and continuously passes the critical horizon, corresponding to (μ_{cr}, T_{cr}) , so that the confinement phase transforms to the deconfinement phase smoothly. In other words, the confinement-deconfinement line is determined by the probe string behavior itself. It is worth to notice that the similar situation takes place in the isotropic case. In the case of the transversal orientation, W_y , the background phase transition line for small μ is located above the phase transition line for the Wilson line, and for small μ we have a smooth confinement-deconfinement phase transition. For $\mu_{yb} < \mu < \mu_{cr}$ we fall in the zone of instability of the background and the first order phase transition takes place.

4 Conclusions

We have found the AdS anisotropic black hole solution for 5-dimensional Maxwell-dilaton gravity that is the generalization of the AGG solution. Our solution includes the non-zero chemical potential and non-trivial warped-factor, thus being a generalization of the AGG-solution.

In our calculations the warped factor is chosen in such a way that the explicit analytical calculations can be performed. This solution can be generalized to provide a more realistic model, but then the solution can be given only in terms of quadratures. We solved the equations of motion to obtain a family of the black hole solutions by modifying the initial potential corresponding to zero temperature. In this construction the special boundary conditions for the dilaton field are chosen, namely we have required that the dilaton field is zero at the horizon.

We have also studied the thermodynamical properties of the constructed black hole background and found the large/small black hole phase transitions at the non-zero temperature. We also got the renorm-group equations and found out that dilaton limits the possible black hole size.

We have studied the behavior of the temporal Wilson loops in the constructed background and obtained confinement/deconfinement phase diagrams for longitudinally and transversally oriented temporal Wilson loops. More detailed consideration for the arbitrary orientation was presented in the talk by Slepov [11, 12].

Further investigations should include the shock-wave and drag-force considerations on our background. We also plan to study $P(z) \sim z^4$ case to reconstruct Cornell potential and develop the renorm-group flow consideration.

References

- [1] I. Aref'eva and K. Rannu, JHEP **05** 206 (2018)
- [2] I. Aref'eva, Phys.Usp. **57** 527 (2014)
- [3] I. Aref'eva, talk "Holography for Heavy Ions Collisions at LHC and NICA" on the XXth International Seminar "Quarks-2018".
- [4] I. Aref'eva, EPJ Web Conf. **164** 01014 (2017)
- [5] I. Aref'eva, A. Golubtsova and E. Gourgoulhon, JHEP **1609** 142 (2016)
- [6] S. He, S.-Y. Wu, Y. Yang and P.-H. Yuan, JHEP **04** 093 (2013)
- [7] Y. Yang and P.-H. Yuan, JHEP **1512** 161 (2015)
- [8] O. Andreev and V. Zakharov, Phys. Rev. D **74** 025023 (2006)
- [9] U. Gursoy, E. Kiritsis, L. Mazzanti and F. Nitti, JHEP **0905**, 033 (2009)
- [10] O. DeWolfe, S. Gubser, C. Rosen and D. Teaney, Prog. Part. Nucl. Phys. **75**, 86 (2014)
- [11] P. Slepov, talk "Holographic study of Wilson loop in the anisotropic background with confinement/deconfinement phase transition" on the XXth International Seminar "Quarks-2018".
- [12] I. Aref'eva, K. Rannu and P. Slepov, arXiv:hep-th/1808.05596 (2018).